AN ORTHOGONAL DECOMPOSITION OF THE AXISYMMETRIC JET MIXING LAYER UTILIZING CROSS-WIRE VELOCITY MEASUREMENTS

by

Mark N. Glauser and William K. George
Turbulence Research Laboratory
Department of Mechanical and Aerospace Engineering
University at Buffalo/SUNY
Buffalo, New York 14260

ABSTRACT

In 1967 Lumley proposed an approach to the objective determination of coherent structures. The method uses an orthogonal decomposition to extract eigenvectors from two point velocity measurements, the lowest order eigenvector representing the largest structure. If the flow is homogeneous, stationary or periodic the general orthogonal decomposition reduces to the familiar harmonic decomposition.

In the current work experiments were performed in the mixing layer of the axisymmetric turbulent jet at x/D=3. These latest experiments extend the earlier work (Glauser and George 1986) to include the radial velocity components. The results presented here show the existence of an azimuthal coherent ring-like structure, dominated by the axisymmetric mode near the potential core but with the fourth, fifth and sixth modes dominating from the center of the mixing layer and outward toward the low-speed side of the mixing layer. The Reynolds stress azimuthal correlations and their breakdown into azimuthal modes show that the incoherent turbulence is transported to the center of the coherent structure as suggested by Hussain (1986). The results are shown to be consistent with the vortex ring-type instability investigated by Widnall and Sullivan (1973).

NOMENCLATURE

A_{ij}	Azimuthal Complex Coefficients
B_{ij}	A_{ij} summed over frequency
m	Azimuthal Mode Number
R_{ij}	Velocity Correlation Tensor
r	Radial Distance Across Jet Mixing Layer
t	Time
u	Velocity Vector
x	Inhomogeneous Spatial Vector
θ	Azimuthal Angle in Jet
λ	Eigenvalues
S_{ij}	Cross Spectral Tensor
ϕ	Eigenvectors
ψ	Eigenvectors in Transformed Domain
ω	Frequency

INTRODUCTION

The earliest investigations of the statistical characteristics of the turbulence in an axisymmetric jet mixing layer were carried out by Laurence (1956), Davies, Barratt and Fisher (1963), and Bradshaw, Ferris and Johnston (1964). Qualitative models for the large scale structures in a number of turbulent flows were formulated by Grant (1958) and Townsend (1956,1970). Crow and Champagne (1971) found identifiable structures in a jet which resembled large scale vortical puffs.

While the precise role of the eddies in the dynamics of the flow has not previously been established, they are suspected of being responsible for the entrainment process in addition to acting as sources of noise. For a review of some of the more recent work on coherent structures see Cantwell (1981), Hussain (1986).

The use of the proper orthogonal decomposition in the identification of coherent structures was first proposed by Lumley (1967) to help identify them in an unambigious manner. An experimental program has been underway at the Turbulence Research Laboratory of the University at Buffalo/SUNY to attempt to generate sufficient data in the turbulent axisymmetric jet to apply the aforementioned decomposition. This program has been performed in phases. The first phase (Glauser et al. 1985, 1987 and Leib et al. 1984) involved measuring simultaneously the instantaneous streamwise velocity at 7 radial locations across the shear layer at x/D=3. The second phase (Glauser and George 1986) involved adding the azimuthal variation to the problem of phase 1. The third phase, which is the subject of this paper, involves adding the radial component of velocity to the problem of phase 2.

The present experiment has generated radial and streamwise cross-spectral data at 8 radial positions and 25 azimuthal positions in the jet mixing layer at x/D=3. These results are compared with those of Glauser and George (1986).

EXPERIMENT AND APPARATUS

The experiment was performed in a circular air jet facility. The jet nozzle was of fifth order polynomial design and has an exit diameter of 0.098m with a contraction ratio of 10:1. The exit conditions of the jet were as follows: The turbulence intensity was 0.35%, the Reynolds number was 110,000 and the boundary layer thickness at the exit ($U = .99\ U_e$) was 0.0012m. Two specially-designed probes containing 4 cross-wire sensors each were situated at x/D=3. The individual sensors (on each rake) were spaced 0.012m apart radially. Measurements were made at 8 radial and 25 azimuthal positions. 1024 time points were taken for each channel giving a time record length of one-half second. 300 such time records were taken at each azimuthal and radial position to insure proper

From this data base $R_{11}(r,r',\tau,\theta)$, $R_{12}(r,r',\tau,\theta)$ and $R_{22}(r,r',\tau,\theta)$ could be computed. The symmetry properties of R_{ij} were utilized to obtain R_{21}.

THE ORTHOGONAL DECOMPOSITION

In 1967 Lumley proposed that the coherent structure should be that structure which has the largest mean square projection on the velocity field. If $\underline{\phi}(\underline{x},t)$ is our candidate structure, then $\underline{\phi}$ should be chosen to maximize

$$\overline{|\underline{u} \cdot \underline{\phi}|^2} = \overline{|a|^2} \tag{1}$$

where $\underline{u} = \underline{u}(\underline{x},t)$ is the instantaneous velocity. The above expression is assumed to be normalized by the modulus of $\underline{\phi}$ so that (1) depends only on the degree of projection and not the magnitude. $\underline{\phi}$ is then, in the averaged mean square sense, the most likely occurrence of $\underline{u}$.

Maximizing $\overline{|\underline{u} \cdot \underline{\phi}|^2}$ leads to the following integral eigenvalue problem:

$$\iint R_{ij}(\underline{x},\underline{x}',t,t')\,\phi^{(n)}{}_j(\underline{x}',t)\,d\underline{x}'dt' = \lambda^{(n)}\phi_i(\underline{x},t) \tag{2}$$

where $R_{ij}(\underline{x},\underline{x}',t,t') = \overline{u_i(\underline{x},t)\,u_j(\underline{x}',t')}$

and $\lambda = |a|^2$.

The Orthogonal Decomposition Theorem reduces to the Harmonic Decomposition Theorem if the direction is stationary, homogeneous or periodic. This implies that these directions must first be removed by Fourier analysis.

In the axisymmetric jet being studied the time 'direction' is stationary and the azimuthal direction is periodic as well as symmetric so that R_{ij} in equation (2) breaks down in the following manner. First the time direction is removed by using the Fourier transform resulting in

$$R_{ij}(\underline{x},\underline{x}',\theta,t) \rightarrow \Phi_{ij}(\underline{x},\underline{x}',\theta,\omega) \tag{3}$$

where Φ_{ij} is the cross-spectral tensor.

A further decomposition (of the cross-spectral tensor now) over the periodic and symmetric direction gives

$$\Phi_{ij}(\underline{x},\underline{x}',\theta,\omega) = \sum_{m=0}^{\infty} A_{ij}(\underline{x},\underline{x}',\theta,m)\cos m\theta \tag{4}$$

where m is the azimuthal mode number and the complex coefficients of the above series are defined by

$$A_{ij}(\underline{x},\underline{x}',\omega,0) = \frac{1}{\pi}\int_0^{\pi} \Phi_{ij}(\underline{x},\underline{x}',\theta,\omega)\,d\theta \tag{5}$$

and by

$$A_{ij}(\underline{x},\underline{x}',\omega,m) = 2/\pi \int_0^{\pi} \Phi_{ij}(\underline{x},\underline{x}',\theta,\omega)\cos m\theta d\theta \tag{6}$$

Now the inhomogeneous direction must be decomposed by using A_{ij} in equation (2).

$$\int A_{ij}(\underline{x},\underline{x}',\omega,m)\,\psi_j^{(n)}(\underline{x}',\omega,m)d\underline{x}' = \lambda^{(n)}(\omega,m)\,\psi_i^{(n)}(\underline{x},\omega,m). \tag{7}$$

The eigenvalues have now become azimuthal mode number dependent eigenspectra

dependent

$$\phi_i^{(n)}(\underline{x},t) \longrightarrow \psi_i^{(n)}(\underline{x},\omega,m). \tag{9}$$

THE PROBLEM SOLVED

A version of the orthogonal decomposition which utilizes the streamwise and radial velocity measurements from the jet can be formulated as

$$\int_R \begin{bmatrix} A_{11}(r,r',\omega,m) & A_{12}(r,r',\omega,m) \\ A_{21}(r,r',\omega,m) & A_{22}(r,r',\omega,m) \end{bmatrix} \begin{bmatrix} \phi_1^{(n)}(r',\omega,m) \\ \phi_2^{(n)}(r',\omega,m) \end{bmatrix} dr' = \lambda^{(n)}(\omega,m) \begin{bmatrix} \psi_1^{(n)}(r,\omega,m) \\ \psi_2^{(n)}(r,\omega,m) \end{bmatrix} \tag{10}$$

where r is the radius in the jet mixing layer. Using the measured values of A_{11}, A_{12}, A_{21} and A_{22} equation (10) can be solved numerically for the eigenvalues and eigenfunctions (Glauser et al. 1987).

RESULTS OF THE AZIMUTHAL DECOMPOSITION ANALYSIS

Before looking at the results of the orthogonal decomposition in the inhomogeneous direction (equation 10) the breakdown into azimuthal modes warrants examination. Writing equations (5) and (6) for A_{11} (the same approach applies for A_{12}, A_{21} and A_{22}).

$$A_{11}(r,r',\omega,0) = \frac{1}{\pi}\int_0^{\pi} \Phi_{11}(r,r',\omega,\theta)\,d\theta \tag{11}$$

and

$$A_{11}(r,r',\omega,m) = \frac{2}{\pi}\int_0^{\pi} \Phi_{11}(r,r',\omega,\theta)\cos m\theta d\theta \tag{12}$$

if both sides of (11) and (12) are summed over ω they become respectively

$$B_{11}(r,r',0) = \frac{1}{\pi}\int_0^{\pi} R_{11}(r,r',\theta)d\theta$$

and

$$B_{11}(r,r',m) = \frac{2}{\pi}\int_0^{\pi} R_{11}(r,r',\theta\cos m\theta d\theta$$

where $R_{11}(r,r',\theta) = \sum_{\omega} \Phi_{11}(r,r',\theta,\omega)$

$$= \overline{u(r',\theta_0)\,u(r',\theta_0+\Delta\theta)}$$

and $B_{11}(r,r',m) = \sum_{\omega} A_{11}(r,r',m,\omega)$.

$R_{11}(r,r',\theta)$ can be reconstructed from the $B_{11}(r,r',m)$ as,

$$R_{11}(r,r',\theta) = \sum_{m=0}^{N-1} B_{11}(r,r',m)\cos m\theta.$$

Equations, similar to the above are also written for A_{12}, A_{21} and A_{22}, hence the corresponding R_{12}, R_{21}, R_{22}, B_{12}, B_{21} and B_{22}.

It is useful to set $r = r'$ so that B_{11}, B_{12}, R_{11}, R_{12}, etc. can be plotted for each radial position in the jet mixing layer. Selected examples of these are plotted in figures 1-8. The following progression across the jet mixing layer begins near the potential core and progresses towards the low speed side of the shear layer.

is clearly a strong correlation over the entire 180 deg. span. The corresponding $B_{11}(m)$ is plotted in Figure 1(b). The 0th mode (axisymmetric mode) can be seen to contain most of the energy indicating a strong ring-like structure at this position.

Figure 2(a) shows measurements of $R_{22}(\theta)$ at the same radial position as above. The radial correlation is seen to go to zero at 90 deg. and then becomes negatively correlated. The corresponding $B_{22}(m)$ is plotted in Figure 2(b). The 1st mode can be seen to dominate in this case. This would indicate either that the ring-like structures flap back and forth or that they are tilted slightly.

Figure 3(a) shows measurements of $R_{12}(\theta)$ at the same radial position as the above. There is clearly a strong correlation over the entire 180 deg. span much the same as was seen in Figure 1. Figure 3(b) shows the corresponding $B_{12}(m)$.

The Center Region of the Mixing Layer

Figure 4(a) shows measurements of $R_{11}(\theta)$ at a position on the high speed side of the shear layer at r/D=0.35. The correlation falls off much more rapidly than that seen in Figure 1(a) indicating the presence of substantially much smaller scale turbulence. The corresponding $B_{11}(m)$ is plotted in Figure 4(b). The 0th mode again dominates but in addition there appears another peak around the 4th, 5th or 6th mode.

Figure 5(a) shows measurements of $R_{22}(\theta)$ at the same radial position as the above at r/D=0.35. This correlation does not go negative like the R_{22} did in Figure 2(a). The corresponding $B_{22}(m)$ is plotted in Figure 5(b). Here the 0th mode comes into play along with the 1st mode as opposed to what was seen in Figure 2(b) where only the 1st mode dominated.

Figure 6(a) shows measurements of R_{12} at the same radial position as the above at r/D=0.35. An interesting thing happens here in that the correlation falls off very fast indicating the predominance of the small structure at this position.This is also seen by examining $B_{12}(\theta)$ shown in Figure 6(b) where the breakdown versus azimuthal modes is seen to be broad band with no distinct peaks. This is quite distinct from the core region where the Reynolds stress is dominated by the 0th mode. The $R_{12}(\theta)$ and $B_{12}(m)$ at r/D=.46 show much the same characteristics as those at r/D=0.35.

Figure 7(a) shows measurements of $R_{11}(\theta)$ at a position just to the high speed sign of the center of the mixing layer, at r/D=.46. The correlation falls off very rapidly. The corresponding $B_{11}(m)$ is plotted in Figure 7(b). An interesting phenomena occurs at this position. Instead of the 0th mode dominating as was seen in Figures 1 and 4, there is a shift here to the 4th, 5th and 6th modes.

Figure 8(a) shows measurements of $R_{12}(\theta)$ at a position just to the low speed side of the center of the jet shear layer at r/D=0.57. Note that there is measurable correlation seen. The corresponding $B_{12}(m)$ is shown in Figure 9(b). Note the preference for the 4th, 5th and 6th modes. Contrast these with those from Figure 6.

The results for $R_{11}(\theta)$, $B_{11}(m)$, $R_{22}(\theta)$ and $B_{22}(m)$ at r/D=0.57 are much the same as those shown in Figures 7 and 5 respectively. $R_{12}(\theta)$ and $B_{12}(m)$ were the only correlations to show significant changes from r/D=.46 as seen by comparing Figures 6 and 8. The remaining correlations at the other positions in the mixing layer, r/D=0.68, r/D=0.79 and r/D=0.9 are not plotted due to lack of space but they also exhibit the

The inhomogeneous problem was solved using Lumley's Orthogonal Decomposition. For each mode number frequency combination (Equation 10) was solved numerically using the measured values of $A_{11}(r,r',\omega,m)$, $A_{12}(r,r',\omega,m)$, $A_{21}(r,r',\omega,m)$ and $A_{22}(r,r',\omega,m)$. The numerical approximation to (10) was discussed by Glauser et al. (1987).

The first three eigenspectra for modes 0 and 1 are shown plotted in Figures 9 and 10. The first eigenspectrum for each mode is seen to dominate (this was the case for the remaining modes also) indicating that one term is adequate, for the description of the large eddy, in the inhomogeneous directions. This is the same result seen in the earlier work (Glauser et al. 1985, 1987).

An additional interesting result can be seen by examining Figures 9 and 10. The peak of $\lambda^1(\omega, 0)$ in Figure 9 is seen to correspond approximately to an exit Strouhal number equal to 0.45 (95 Hz). This is higher than the value of 0.3 which is given by some authors (see for example Crow and Champagne 1971). When examining Figure 10, however, $\lambda^1(\omega,1)$ is seen to peak around an exit Strouhal number of 0.25. This would suggest that the Strouhal number of 0.3 represents an average over the first two azimuthal modes which, in fact, comprise 90% of the total energy. If so, the orthogonal decomposition used here would seem to have a real advantage over the earlier techniques in that it can distinguish clearly these phenomena.

DISCUSSION

The preference for the 4th, 5th and 6th modes as seen in Figures 7 and 8 is intriguing. A 6th lobe preference (although weak) was seen by Sreenivasan (1984) at a position closer to the potential core at x/D=1. A detailed stability analysis for vortex rings has been carried out by Widnall and Sullivan (1973). From this analysis the number of preferential lobes is seen to depend on the circulation as well as on the ratio of the vortex core radius to the ring radius. Neither of these terms are known in the present jet with any confidence but the 6th lobe preference noticed here is not inconsistant with the results from Widnall and Sullivan (1973).

An additional point of considerable interest is the fact that the uv azimuthal correlation are strongly correlated near the potential core (see Figure 3), become broadband as one proceeds toward the center of the mixing layer (see Figure 6), and then become more correlated as one proceeds toward the outside of the shear layer (see Figure 8). This indicates either that the incoherent turbulence is convected toward the center of the large structure, or is generated there.

A Proposed Mechanism

The previous discussion suggest the following mechanism for turbulence production which consists of four stages. These four stages are shown in Figure 11. Vortex ring-like concentrations arise from an instability of the base flow, the induced velocities from vortices which have already formed providing the perturbation for those which follow. These pairs of rings then behave like the text book examples of inviscid rings, the rear vortex ring overtaking the vortex ring ahead of it, the rearward vortex being reduced in radius and the forward are being expanded by their mutual interaction. The rearward ring is stabilized by the reduction in its vorticity (by compression) thus the predominance of the 0th mode on the high speed side (core region). The forward ring has its vorticity increased by stretching as it expands in radius. This narrowing of its core while the radius is expanding causes the vortex to become

forward one and the now highly distorted ring interaction with itself, accelerates the instability until its vorticity is now entirely in small scale motions, in effect an energy cascade from modes 4-6 all the way to dissipative scales. This incoherent turbulence is swept from the outside where it has been carried, back to the center of the mixing layer as the still intact rearward vortex passes. It is this collecting of the debris, both small scale vorticity and fluid material, which has been recognized as "pairing". Thus pairing is not a mechanism as has often been claimed, but simply a phenomenon which marks the end of the life cycle of a large eddy. The entire process is repeated as a new rearward vortex overtakes and destabilizes the one ahead of it.

The above sequence is consistent with all of the observations of this experiment and those of others (v. Hussain 1986). The only missing piece of information is to experimentally establish the sequencing of the events, a task for a future decomposition which will include the streamwise variable dependence (i.e. x).

CONCLUSION

The basic features of the azimuthal large structure were the same as those obtained with the streamwise ONLY correlation (Glauser and George, 1986), in particular the strong correlation and dominance of the 0th mode near the potential core and the preference for the 4th, 5th and 6th modes elsewhere. This would imply that, as far as the large scale structure is concerned that the streamwise azimuthal correlations would be an adequate description. The addition of the Reynolds stress and radial azimuthal correlations, however, give additional insight into what is happening across the shear layer, in particular, the mechanism of the breakup of the structure.

The eigenspectra extracted using this latest data base show the same basic characteristics as those extracted from the streamwise only decomposition (Glauser and George 1986). The shapes of the particular eigenspectra are essentially identical. The only measurable difference between the eigenspectra is in their respective amplitudes, those from the latest data being higher. This is to be expected because the eigenspectra are essentially the total energy integral across the shear layer, and with this latest data there is the additional contribution to the total energy from the v component of velocity.

A mechanism for the life cycle of coherent structures and for turbulence production in the axisymmetric jet mixing layer has been proposed which accounts for the observed phenomena and is amenable to dynamical analysis using the equations of motion. It will be interesting to see if the details can in fact, be confirmed by a direct application of the decomposition to the equations of motion. If so, we may at long last have a detailed example of how Reynolds stress acts to remove energy from the mean flow and distributes it to all scales of motion.

ACKNOWLEDGEMENTS

This research was initiated under support from the National Science Foundation under Grant No. ENG7617406 and the Air Force Office of Scientific Research under Contract Nos. F49620780C0047 and F4962080C0053. Work has continued under NSF Grant No. MSM8316833 and with the support of the NASA trainee program for Mark Glauser at NASA Ames. We gratefully acknowledge the technical support and continuing interest of Parviz Moin at Stanford/NASA Ames.

Bradshaw, P., Ferris, D.H., Johnson, R.F. (1964) Turbulence in the Noise-Producing Region of a Circular Jet. J. Fluid Mech. 19, 591.

Cantwell, B.J. (1981) Organized Motion in Turbulent Flow. Ann. Rev. Fluid Mech. 13, 457.

Crow, S.C., Champagne, F.H. (1971) Orderly Structure in Jet Turbulence J. Fluid Mech. 48, 547.

Davies, P.O.A.L., Barratt, M.J., Fisher, M.J. (1963) The Characteristics of Turbulence in the Mixing Region of a Round Jet. J. Fluid Mech. 15, 337.

Glauser, M.N., Leib, S.J. and George, W.K. (1985) Coherent Structures in the Axisymmetric Jet Mixing Layer. Proc. of 5th Symposium Turbulent Shear Flow Conference, Cornell University.

Glauser, M.N., Leib, S.J. and George, W.K. (1987) Coherent Structures in the Axisymmetric Jet Mixing Layer. Turbulent Shear Flows 5, Springer-Verlag.

Grant, H.L. (1958) The Large Eddies of Turbulent Motion, J. Fluid Mech. 4, 149.

Hussain, A.K.M.F. (1986) Coherent Structure and Turbulence. J. Fluid Mech. Vol. 173, 303-356.

Laurence, J.C. (1956) Intensity, Scale and Spectra of Turbulence in Mixing Region of Free Subsonic Jet. NACA Report No. 1292.

Leib, S.J., Glauser, M.N. and George, W.K. (1984) An Application of Lumley's Orthogonal Decomposition to the Axisymmetric Turbulent Jet Mixing Layer. Proceedings 9th Rolla Symposium.

Lumley, J.L. (1967) The Structure of Inhomogeneous Turbulent Flows. In Atm. Turb. and Radio Wave. Prop., (Yaglom and Tatarsky, ed.) Nauka, Moscow, 166-178.

Sreenivasan, K.R. (1984) The Azimuthal Correlations of Velocity and Temperature Fluctuations in an Axisymmetric Jet. Phys. Fluids 27 (4).

Townsend, A.A. (1956) The Structure of Turbulent Shear Flow (Cambridge University Press).

Townsend, A.A. (1976) 2nd Ed. The Structure of Turbulent Shear Flow (Cambridge University Press).

Widnall, S.E., Sullivan, J.P. (1973) Proc. R. Soc. London Ser. A332, 335.

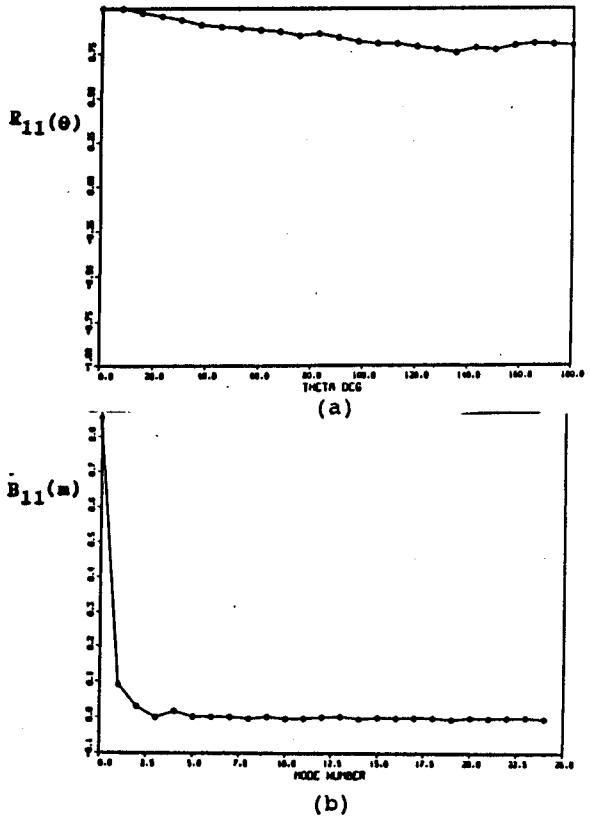

Figure 1 (a) $R_{11}(\theta)$ at r/D=0.13, x/D=3
(b) $B_{11}(m)$ at r/D=0.13, x/D=3

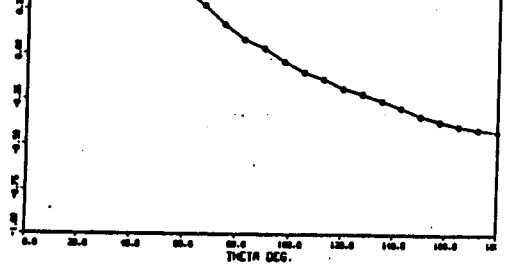

(a)

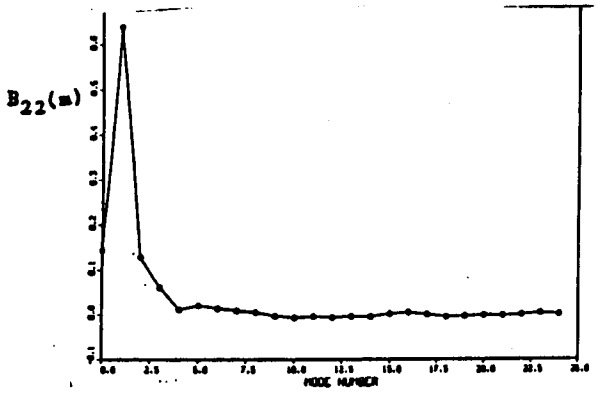

(b)

Figure 2 (a) $R_{22}(\theta)$ at r/D=0.13, x/D=3
(b) $B_{22}(m)$ at r/D=0.13, x/D=3

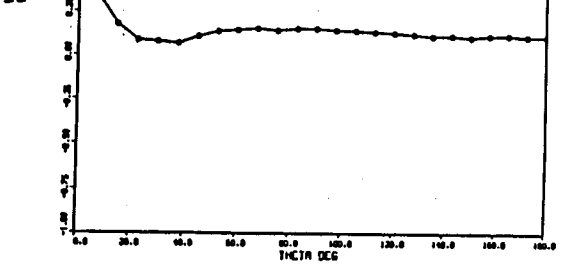

(a)

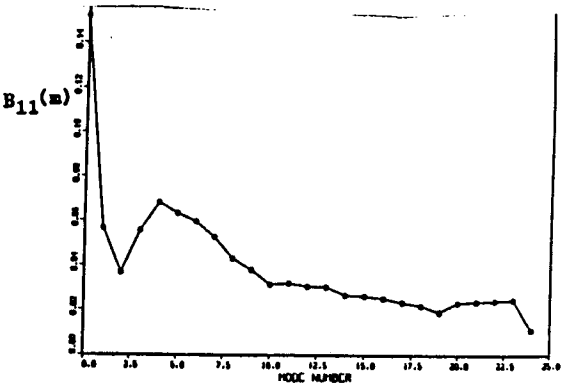

(b)

Figure 4 (a) $R_{11}(\theta)$ at r/D=0.35, x/D=3
(b) $B_{11}(m)$ at r/D=0.35, x/D=3

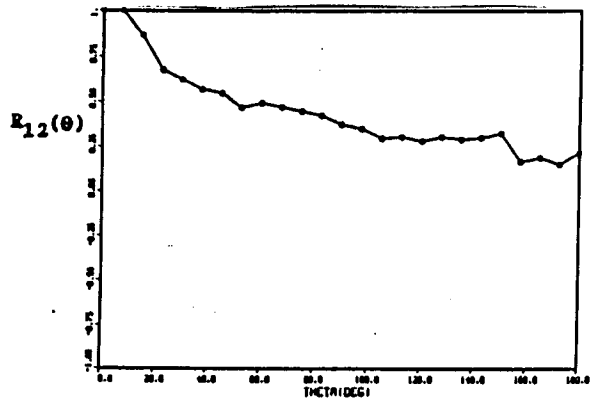

(a)

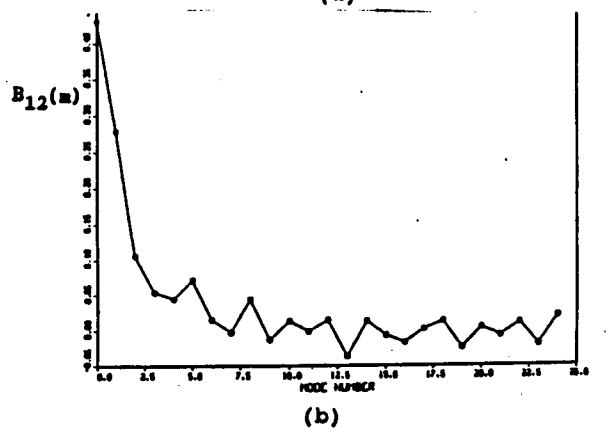

(b)

Figure 3 (a) $R_{12}(\theta)$ at r/D=0.13, x/D=3
(b) $B_{12}(m)$ at r/D=0.13, x/D=3

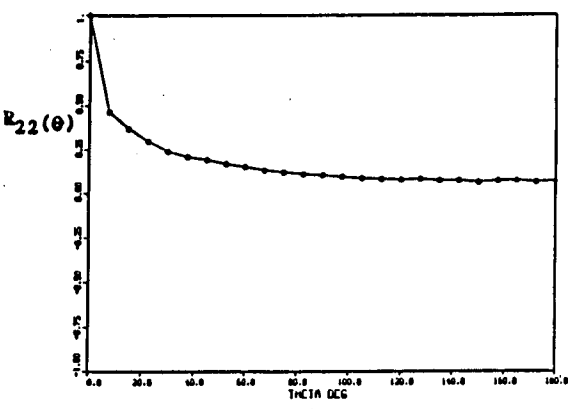

(a)

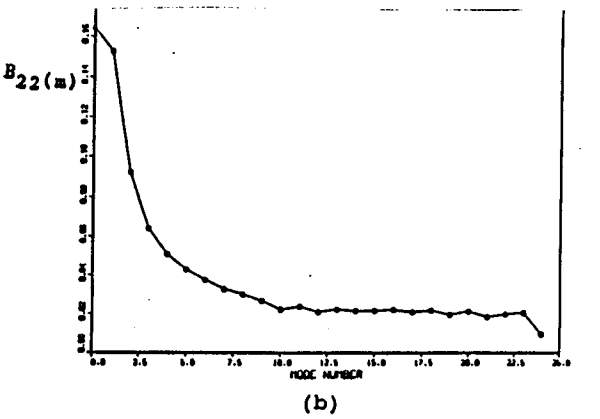

(b)

Figure 5 (a) $R_{22}(\theta)$ at r/D=0.35, x/D=3
(b) $B_{22}(m)$ at r/D=0.35, x/D=3

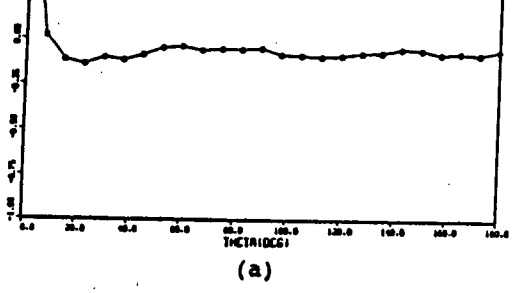

(a)

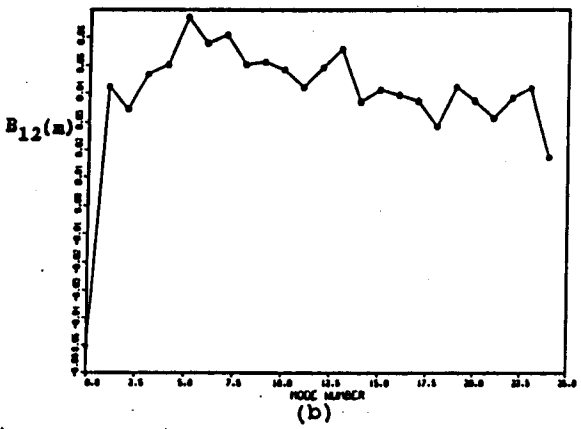

(b)

Figure 6 (a) $R_{12}(\theta)$ at r/D=0.35, x/D=3
(b) $B_{12}(m)$ at r/D=0.35, x/D=3

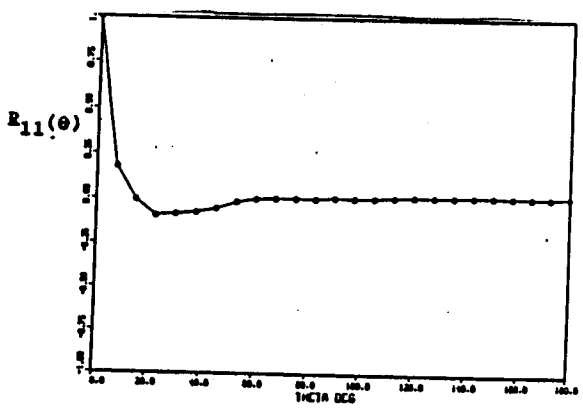

(a)

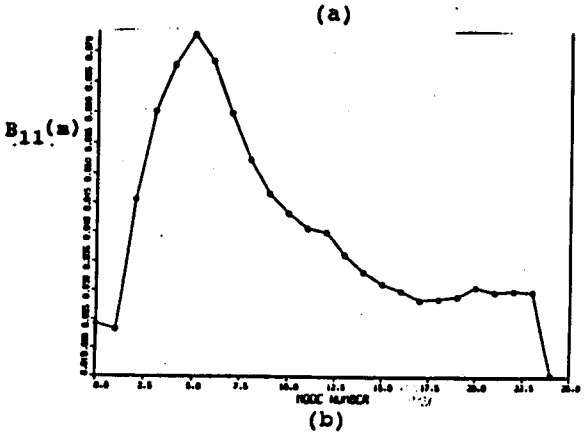

(b)

Figure 7 (a) $R_{11}(\theta)$ at r/D=0.46,x/D=3
(b) $B_{11}(m)$ at r/D=0.46, x/D=3

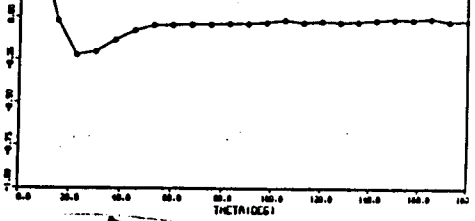

(a)

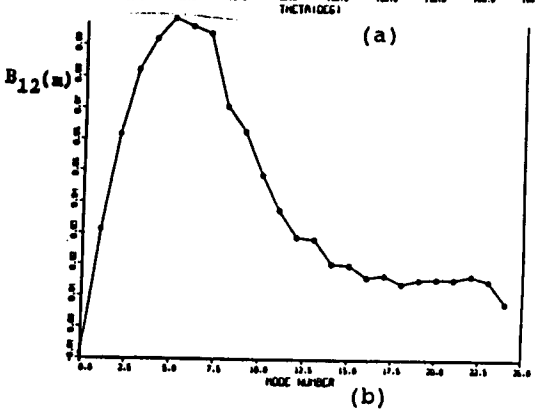

(b)

Figure 8 (a) $R_{12}(\theta)$ at r/D=0.57, x/D=3
(b) $B_{12}(m)$ at r/D=0.57, x/D=3

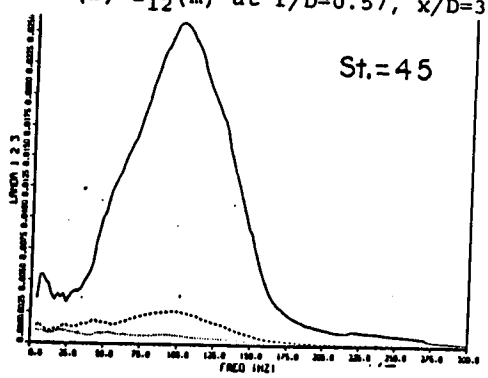

Figure 9

First 3 eigenspectra mode 0. Note the peak in the first eigenspectrum at a Strouhal #=.45

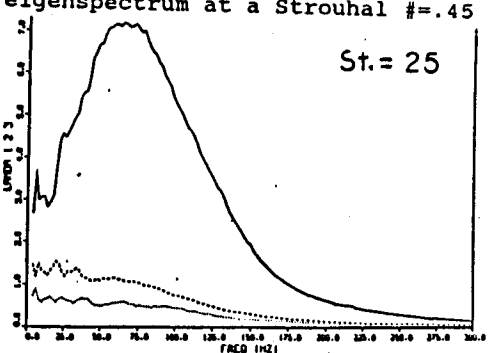

Figure 10

First 3 eigenspectra, mode 1, Note the peak in the first eigenspectum at a Strouhal #=.25

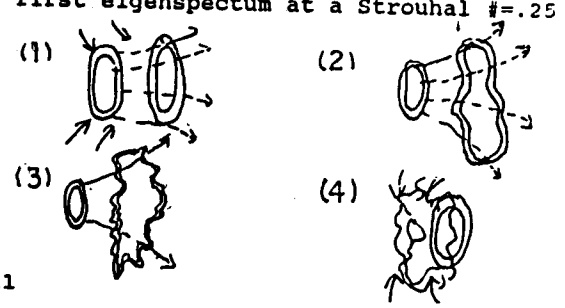

Fig. 11

The proposed 4 stages of turbulence production.